



# Post-Stroke Microglia Induce Sirtuin2 Expression to Suppress the Anti-inflammatory Function of Infiltrating Regulatory T Cells

Long Shu,<sup>1</sup> Chao-qing Xu,<sup>1</sup> Zhao-Yi Yan,<sup>1</sup> Yang Yan,<sup>1</sup> Shi-Zhu Jiang,<sup>2</sup> and Ying-Rui Wang<sup>1,3</sup>

**Abstract**— Ischemic stroke is among the leading causes of death and disability across the globe. Post-stroke neuroinflammation contributes to the pathophysiology of ischemic stroke in the acute phase through damaging neurons in the penumbra region. Infiltrating regulatory T cells (Treg cells) provide neuronal protection in ischemic brains. In the current study using a mouse-transient middle cerebral artery occlusion (MCAO) model, we characterized the changes of sirtuin expression in infiltrating Treg cells in the acute phase of ischemia. We found that Sirt2 was remarkably upregulated in infiltrating Treg cells at day 3 post-MCAO. *In vitro* inhibition of Sirt2 activity enhanced the expression of immunosuppression-associated molecules including forkhead box P3 (Foxp3) in Treg cells. Using a lentiviral system to express exogenous Sirt2 in Treg cells, we found that Sirt2 weakened the anti-inflammatory effect of Treg cells on pro-inflammatory macrophages. Additionally, post-MCAO microglia increased Sirt2 expression in Treg cells in a cell-to-cell contact manner. We further found that microglia remarkably induced hypoxia-inducible factor 1-alpha (HIF-1 $\alpha$ ) expression in Treg cells, and inhibition of HIF-1 $\alpha$  abolished microglia-induced Sirt2 upregulation. Collectively, we discovered a novel mechanism by which the immunoregulatory activity of infiltrating Treg cells is modulated after ischemia.

**KEY WORDS:** ischemic stroke; regulatory T cells; sirtuin; hypoxia-inducible factor 1-alpha; microglia.

**Electronic supplementary material** The online version of this article (<https://doi.org/10.1007/s10753-019-01057-3>) contains supplementary material, which is available to authorized users.

<sup>1</sup> Department of Neurology, Affiliated Renhe Hospital of China Three Gorges University, Yichang City, 443000, Hubei Province, China

<sup>2</sup> Department of Digestive Diseases, Affiliated Renhe Hospital of China Three Gorges University, Yichang City, 443000, Hubei Province, China

<sup>3</sup> To whom correspondence should be addressed at Department of Neurology, Affiliated Renhe Hospital of China Three Gorges University, Yichang City, 443000, Hubei Province, China. E-mail: 33266565@qq.com

## INTRODUCTION

Ischemic stroke is one of the leading causes of death and disability worldwide. Post-stroke neuroinflammation, which features infiltration of peripheral leukocyte into the brain parenchyma, microglia activation, and release of pro-inflammatory mediators, contributes to the pathophysiology of ischemic stroke [1]. Neuroinflammation leads to secondary injury of neurons in the penumbra region [2]. Infiltrating T cells could impact the ischemic lesion both dependently and independently of antigen-specificity [3, 4]. In particular, forkhead box P3 (Foxp3)-positive

regulatory T cells (Treg cells) are believed to counteract acute neuroinflammation and protect neurons from the secondary injury [5, 6]. However, the molecular mechanisms by which the function of infiltrating Treg cells is modulated have not been thoroughly elucidated.

The sirtuin family comprises seven members (Sirt1–7), which act as NAD<sup>+</sup>-dependent protein deacetylases and/or ADP-ribosylases [7]. They are involved in the control of cellular pathways, including metabolism, stress, and genome stability. The roles of sirtuins in the immune system has been recently disclosed. In the context of T cell biology, Sirt1-deficiency increases T cell activation and the development of Th17-associated autoimmune diseases [8]. Activation of Sirt1 reduces T cell activation [9]. Importantly, Sirt1 deletion promotes the expression of Foxp3 and increases Treg suppressive function [10]. Consistently, Sirt1 results in Foxp3 proteasomal degradation, while Sirt inhibition increases Foxp3 transcriptional activity [11, 12]. Hence, Sirt1 is a negative regulator of T cell functions including Treg function. However, the effects of other sirtuins on Treg cells have not been studied. Moreover, whether sirtuins modulate the functions of infiltrating Treg cells in post-stroke brains remains unknown.

In the current study, we characterized the changes of sirtuin expression in infiltrating Treg cells in the acute phase of transient middle cerebral artery occlusion (MCAO). We found that Sirt2 was significantly upregulated in infiltrating Treg cells in a time-dependent manner. *In vitro* inhibition of Sirt2 activity enhanced the expression of immunosuppression-associated molecules in Treg cells. Additionally, post-MCAO microglia increased Sirt2 expression in Treg cells in a cell-to-cell contact manner. Microglia remarkably induced hypoxia-inducible factor 1- $\alpha$  (HIF-1 $\alpha$ ) expression in Treg cells, and inhibition of HIF-1 $\alpha$  abolished microglia-induced Sirt2 upregulation. Our research could provide a new clue for designing anti-neuroinflammation treatments after ischemic stroke.

## MATERIALS AND METHODS

### Mice

Animal experiments were approved by China Three Gorges University Animal Care and Use Committee, and were conducted in compliance with the Animal Research: Reporting of *In Vivo* Experiments (ARRIVE) guidelines. Three hundred 6–8-week-old male Foxp3-GFP transgenic mice (C57BL/6J background, originally from Jackson Lab

and 250 wild type C57BL/6J mice were obtained from the Animal Center of Renmin Hospital of Wuhan University. The mice were housed at 22 ± 2 °C in the pathogen-free animal facility of China Three Gorges University with a 14-h light/10-h dark cycle and 40% humidity. The mice were fed with autoclaved diet containing 6% fat. The bedding was autoclaved and changed every 1 week.

### Transient MCAO Model

The mice were randomly divided into sham group and MCAO group (including day 1, day 3 and day 5 group). Transient MCAO was conducted following the previous protocol [13]. Briefly, the mice were anesthetized *via* inhalation of 2.0% isoflurane and maintained by inhalation of 1.0% isoflurane in 70% N<sub>2</sub>O and 30% O<sub>2</sub> using the V-10 Anesthesia system (VetEquip, Inc.). The body temperature was monitored by a rectal probe and was maintained at 36.5–37.5 °C with a thermostat-controlled heating blanket. The fur on the ventral neck area was shaved with clippers to expose the skin. The surgical region was disinfected using 70% ethanol. Under a microdissection microscope (Nikon), a 1-cm-long midline incision was made on the neck. The common carotid artery, external carotid artery, and internal carotid artery (ICA) were dissected from the surrounding connective tissues and nerves. A silicon-coated 6-0 nylon monofilament was inserted into the left ICA and advanced until it occluded the origin of the middle cerebral artery (MCA). The MCA was occluded for 90 min followed by reperfusion through suture withdraw. Cerebral blood flow was monitored prior to and after MCAO-reperfusion using a laser Doppler flowmetry (ADInstruments). A total of 522 mice were subject to MCAO surgery. Among them, 377 mice were recruited in the study since they had a residual cerebral blood flow less than 20% of original levels during occlusion, cerebral blood flow more than 80% of original levels within 10 min of reperfusion, and survived for at least 3 days after MCAO. One hundred forty-four mice were excluded because they died within 3 days after MCAO, or their cerebral blood flow was unsatisfactory during occlusion or after reperfusion. The sham mice received the same procedure without the insertion of sutures. The MCAO model performer and leukocyte analyzers were double blinded.

### Isolation of Leukocytes from Peripheral Blood, Spleens, and Ipsilateral Hemispheres

At days 1, 3, and 5 after MCAO, each mouse was anesthetized through isoflurane inhalation. The peripheral

blood was collected from the tail vein, and red blood cells were lysed using Tris-NH<sub>4</sub>Cl buffer. Blood leukocytes were resuspended in phosphate-buffered saline (PBS) for further tests. The mouse splenic leukocytes were prepared by pressing the spleens through 70- $\mu$ m cell strainers, followed by red blood cell lysis with Tris-NH<sub>4</sub>Cl buffer. To obtain the infiltrating leukocytes in post-MCAO brains, each mouse was intra-cardiacally perfused with 20 ml of ice-cold PBS. The ipsilateral hemisphere was taken and cut into approximately 1-mm<sup>3</sup> pieces, followed by digestion with 1 ml of digestion solution (RPMI1640 containing 0.5 mg/ml collagenase IV, 100  $\mu$ g/ml DNase I, and 5 mM CaCl<sub>2</sub>) for 30 min at 37 °C. The digested tissue was filtered through a 70- $\mu$ m cell strainer to prepare a tissue homogenate. The homogenate was then mixed with 4 volumes of 30% Percoll (GE Healthcare) and was loaded onto an equal volume of 70% Percoll. After that, the sample was centrifuged at 500 $\times$ g for 15 min. Cells in the interface between 30 and 70% Percoll were harvested and resuspended in ice-cold PBS before further tests.

### Flow Cytometry

The following antibodies were purchased from Biogegend: APC anti-TCR $\beta$  (H57-597), Percp anti-CD4 (GK1.5), PE anti-ICOS (15F9), PE-Cy7 anti-CTLA-4 (UC10-4B9), APC-Cy7 anti-CD45 (30-F11), and PE-Cy7 anti-CD11b (M1/70).  $5 \times 10^5$ -ml cells were stained with 5  $\mu$ g/ml of each antibody on ice for 20 min before analysis on a BD FACSCalibur<sup>TM</sup> cytometer. For cell sorting, stained cells were enriched using a BD InFlux Cell Sorter.

### RNA Purification, cDNA Synthesis, and Real-Time PCR

The reagents were purchased from Thermo Fisher. Total RNAs were purified with Arcturus PicoPure RNA Isolation Kit. RNAs were reversely transcribed to cDNAs using SuperScript<sup>®</sup> III First-Strand Synthesis System following the manufacturer's instructions. Real-time PCR was conducted using Fast SYBR Green Master Mix on a 7300 Real-Time PCR System (Invitrogen). Data were analyzed with the 7300 system software. Primer sequences were shown in Table 1.

### Lentiviral Preparation and Transduction

The mouse Sirt2 lentiviral vector was purchased from Applied Biological Materials (ABM) Inc. This vector contains Sirt2 and GFP coding sequences. To produce the lentiviruses,  $5 \times 10^5$  HEK293T cells were incubated in a

10-cm culture dish overnight until 80% confluency. Cells were pretreated with 10  $\mu$ M chloroquine diphosphate (Sigma-Aldrich) for 3 h. After that, 0.65 pmol pRSV-Rev (Addgene), 1.2 pmol pMDLg/pRRE (Addgene), 1.5 pmol lentiviral vector, and 80  $\mu$ g polyethylenimine (Sigma-Aldrich) were mixed in 1 ml of Opti-MEM. The mixture was then used to incubate HEK293T cells overnight. The medium was changed in the next morning. On day 2 and day 3 after transfection, the supernatants were collected, centrifuged at 500g for 5 min, and filtered through 0.45- $\mu$ m filters. The lentiviruses were enriched with Lenti-X<sup>TM</sup> Maxi Purification Kit (Clontech). The viral titer was assessed using Lenti-X qRT-PCR Titration Kit (Clontech). The lentivirus expressing Sirt2 was named L-S, while the control lentivirus without Sirt2 sequence was named L-C.

To transduce Treg cells, splenic CD4<sup>+</sup>CD25<sup>+</sup> T cells were isolated from normal C57BL/6 male mice using Dynabeads<sup>TM</sup> FlowComp<sup>TM</sup> Mouse CD4+ CD25+ Treg Cells Kit (Thermo Fisher) following the vendor's protocol.  $1 \times 10^6$ /ml CD4+ CD25+ T cells were stimulated *in vitro* for 24 h with 5  $\mu$ g/ml plate-bound CD3 mAb, 1  $\mu$ g/ml soluble CD28 mAb, and 10 ng/ml rmIL-2 (All from BD Biosciences). The medium was replaced by fresh medium containing 5  $\mu$ g/ml polybrene. Then, cells were transduced with lentivirus at the MOI of 10 overnight. Cells were maintained for 2 days with plate-bound anti-CD3 antibody and soluble anti-CD28 antibody plus rmIL-2.

### Cell Culture

Infiltrating GFP<sup>+</sup> Treg cells were sorted and pooled from 10 to 12 mouse brains by flow cytometry.  $1 \times 10^5$ -ml-sorted Treg cells were incubated with 5  $\mu$ g/ml plate-bound CD3 mAb (145-2C11, BD Biosciences), 1  $\mu$ g/ml soluble CD28 mAb (37.51, BD Biosciences), and 10 ng/ml rmIL-2 (BD Biosciences) for 24 h in the presence or absence of 10  $\mu$ M Sirt2 inhibitor AGK2 (Sigma-Aldrich). After that, cells were subject to RNA purification, cDNA synthesis, and real-time PCR.

To check the anti-inflammatory effect of Treg cells, F4/80<sup>+</sup> macrophages were sorted from normal mouse spleens and were maintained in supplemented RPMI1640.  $1 \times 10^5$ /ml macrophages were stimulated for 6 h with lipopolysaccharide (LPS, 50 ng/ml, Sigma). Macrophages were then washed with PBS once and co-cultured with  $5 \times 10^5$ /ml lentivirus-transduced Treg cells in 96-well V-bottom microplates in the presence of plate-bound CD3 mAb and soluble CD28 mAb. After 24-h co-culture, cells were

**Table 1.** Primer Sequences for Real-Time PCR

Molecule	Forward (5' to 3')	Reverse (5' to 3')
Sirt1	TACCTTGGAGCAGGTTGCAG	GCTTCATGATGGCAAGTGGC
Sirt2	TTTGGTGGGAGCCGGAATC	CCAGGTTTGCATAGAGGCCA
Sirt3	TCCGGGAGGTGGGAGAAG	CACCATGACCACCACCTAC
Sirt4	TGAAAGAGGCGGACTCCCTA	CAGGCAAGCCAAATCGTCA
Sirt5	ACTTCTTAACCGCCCTGTGG	TTGGGGCTTGAAGGGTGTIT
Sirt6	GCCCAACAGCCCTATACTCC	TGTGGTTCCTCAAGTCCCC
Sirt7	TCTACAACCGTGGCAGGAT	AGTGACTTCTACTGTGGCTG
Ebi3	TCTGCCGGTTCATCCCTCA	GGCGAAAGCGAACATGTGAAT
GITR	CTCGAGAGACCCAGCCATTC	CCTCAGGGAACCTGGAAGCTG
CD39	AATGAGGTCCATTTGCGGCT	TTGGGTGGAGTAGCCCTTTG
ICOS	TGACCCACCTCCTTTTCAAG	TTAGGGTCATGCACACTGGA
CTLA-4	GGACGCAGATTTATGTCATTGATC	CCAAGTAACTGCGACAAGGA
IL-10	AGGCGCTGTCATCGATTCT	ATGGCCTTGTAGACACCTTGG
IL-12a	CACAAGAACGAGAGTTGCCT	TAAGGGTCTGCTTCTCCAC
TGF- $\beta$ 1	CTGCTGACCCCACTGATAC	TGAGCGCTGAATCGAAAGC
TNF- $\alpha$	TCGGTCCCAACAAGGAGGAG	GGGCTTGTCACTCGAGTTTTG
IL-1 $\beta$	TGTCTGACCCATGTGAGCTG	GCCACAGGGATTTTGTGCTT
IL-6	ACTTCACAAGTCGGAGGCTT	TTCTGACAGTGCATCATCGCT
iNOS	CGAAACGCTTCACTTCCAA	TGAGCCTATATTGCTGTGGCT
Actin	GATGGTGAAGGTCGGTGTGA	TGAACCTGCCGTGGGTAGAG

dissociated with 5-min treatment of Trypsin-EDTA Solution (Sigma). GFP<sup>-</sup> cells, *i.e.*, macrophages were sorted by flow cytometry and subject to further tests.

To determine the Sirt2-inducing factors, CD45<sup>high</sup>CD11b<sup>+</sup> macrophages and CD45<sup>low</sup>CD11b<sup>+</sup> microglia were enriched from 5 pooled ipsilateral hemispheres of mouse brains. They were cultured at the density of  $1 \times 10^6$ /ml in supplemented RPMI1640. They were then co-cultured with the equal volume of  $1 \times 10^5$ /ml splenic Treg cells for 24 h in the presence of 10 ng/ml rmIL-2. In separation culture, macrophages or microglia were seeded in the lower chambers of a 96-well HTS Transwell plate (Corning), while Treg cells were seeded in the inserts (membrane pore size = 0.4  $\mu$ m). In some experiments, Treg cells were pretreated with 20  $\mu$ M HIF-1 inhibitor PX-478 for 4 h prior to co-culture with microglia.

### Western Blot

Cells were lysed with RIPA buffer (Abcam) containing the proteinase inhibitor cocktail (Abcam). The protein concentrations were quantified using the Pierce BCA Protein Assay Kit (Thermo Fisher). A total of 10  $\mu$ g proteins of each sample was loaded. The following antibodies (Santa Cruz Biotechnology)

were used:  $\beta$ -actin antibody (sc-47778), Sirt2 antibody (sc-28298), HIF-1 $\alpha$  antibody (sc-13515), HIF-2 $\alpha$  antibody (sc-13596), Foxo1 antibody (sc-374427), Foxo3 antibody (sc-48348), Foxp3 antibody (2A11G9), horseradish peroxidase-conjugated goat anti-mouse IgG. The signal was developed using SuperSignal<sup>TM</sup> West Femto Maximum Sensitivity Substrate (Thermo Fisher) and was scanned by the BioSpectrum Imaging System (UVP, LLC).

### Statistics

Data were presented as means  $\pm$  standard deviation. The unpaired *t* test or one-way ANOVA with post hoc Tukey HSD test was conducted for comparison of mean values among groups. To achieve the statistic power of 0.8 and type I error rate of 0.05, the sample size of each experiment was determined by the online tool ([www.powerandsamplesize.com/Calculators/](http://www.powerandsamplesize.com/Calculators/)) using formula  $[1 + 1/\kappa] \times [\sigma \times (z_{1-\alpha/2} + z_{1-\beta})/\mu_A - \mu_B]^2$  for *t* tests, and  $2 \times [\bar{\sigma}(z_{1-\alpha/2} + z_{1-\beta})/(\mu_A - \mu_B)]^2$  for one-way ANOVA tests.  $\kappa$  is the matching ratio.  $\bar{\sigma}$  is standard deviation.  $\alpha$  is type I error.  $\tau$  is the number of comparisons to be made.  $\mu$  is the mean in the pilot study. Each experiment was independently repeated 2 or 3 times. *p* value < 0.05 was considered statistically significant.



## RESULTS

### The Expression of Sirtuins in Infiltrating Treg Cells After MCAO

To characterize the expression of sirtuins in Treg cells, leukocytes were isolated from peripheral blood and ipsilateral hemispheres after MCAO. Dead cells were excluded *via* PI staining (Fig. S1), and T cells were distinguished through TCR staining (Fig. S2). Infiltrating T cells were increased in ipsilateral hemispheres while the proportion of blood T cells was not profoundly changed (Fig. S2). Very rare T cells were found in sham-operated brains (Fig. S2). The infiltrating T cells contained a substantial population of CD4<sup>+</sup>GFP<sup>+</sup> cells (*i.e.*, Treg cells) at each indicated time point, and the proportion of infiltrating Treg cells peaked at day 3 post-MCAO (Fig. 1a). We then assessed the mRNA abundances of sirtuins in blood or infiltrating Treg cells. As indicated in Fig. 1b to d, the mRNA abundances of Sirt1, Sirt2, and Sirt6 were significantly altered in infiltrating Treg cells but not blood Treg cells. Notably, in these infiltrating Treg cells, the mRNA levels of Sirt2 and Sirt6 were initially decreased at day 1 after MCAO and were subsequently increased at day 3 after MCAO in comparison with their levels in blood Treg cells. Sirt2 expression exhibited the most dramatic increase at day 3. The increase of Sirt2 expression was confirmed by Western blot (Fig. S3). No significant changes in the mRNA levels of Sirt3, Sirt4, Sirt5, and Sirt7 were observed (Fig. S4).

### Sirt2 Impairs the Immunoregulatory Activity of Treg Cells

We first checked the expression of immunosuppression-related molecules in infiltrating Treg cells. As shown in Fig. 2a, b, infiltrating Treg cells expressed the highest inducible costimulator (ICOS) and cytotoxic T lymphocyte-associated antigen 4 (CTLA-4) at day 1 after MCAO, while ICOS and CTLA-4 expression was remarkably decreased at day 3 and was partially recovered at day 5 after MCAO. We also evaluated the production of two anti-inflammatory cytokines, *i.e.*, interleukin 10 (IL-10) and transforming growth factor beta (TGF- $\beta$ ) in infiltrating Treg cells. It turned out that IL-10 expression had a similar pattern to ICOS and CTLA-4 (Fig. 2c). Hence, it seemed that the expression of these molecules was negatively correlated with Sirt2 expression.

We then sorted infiltrating GFP<sup>+</sup> Treg cells from ipsilateral hemispheres at day 3 post-MCAO, and stimulated them with agonistic antibodies for 24 h in the presence or absence of Sirt2 inhibitor AGK2. After that,

the expression of immunosuppression-related molecules was assessed *via* real-time RT-PCR. As shown in Fig. 2d and Fig. S5, stimulation with agonistic antibodies profoundly promoted the expression of all molecules tested, whereas AGK2 further increased the expression of ICOS, CTLA-4, TGF- $\beta$ , and Epstein-Barr virus-induced gene 3 (Ebi3). Furthermore, after antibody stimulation, AGK2-treated Treg cells had higher GFP intensity than vehicle-treated Treg cells (Fig. 2e). Collectively, our data suggest that Sirt2 inhibits the expression of ICOS, CTLA-4, TGF- $\beta$ , Ebi3, and Foxp3.

### Exogenous Sirt2 Suppresses the Anti-inflammatory Activity of Treg Cells

To further confirm the effect of Sirt2 on Treg cell function, normal mouse splenic Treg-enriched cells were transduced with lentivirus encoding Sirt2 and GFP. As shown in Fig. 3a, over 40% of Treg cells were GFP<sup>+</sup> at day 2 after transduction, suggesting that the transduction efficiency was acceptable. The transduction with L-S (lentivirus encoding Sirt2) substantially promoted Sirt2 expression but decreased Foxp3 expression, as compared with mock transduction and L-C (control lentivirus) transduction (Fig. 3b). Expression of exogenous Sirt2 did not alter Treg cell apoptosis (Fig. 3c and Fig. S6). Furthermore, L-S-transduced Treg cells produced lower anti-inflammatory cytokines such as IL-10, TGF- $\beta$ , and IL-12a (Fig. 3d). We then co-cultured lentivirus-transduced Treg cells with LPS-stimulated splenic macrophages to check the anti-inflammatory activity of Treg cells. As demonstrated in Fig. 3e, in comparison with L-C-transduced Treg cells, L-S-transduced Treg cells were less potent in suppressing the expression of IL-1 $\beta$ , TNF- $\alpha$ , IL-6, and iNOS in activated macrophages. Hence, Sirt2 inhibits the suppressive effect of Treg cells on pro-inflammatory macrophages.

### Post-MCAO Microglia Induce Sirt2 Expression in Treg Cells

To determine which factor induces Sirt2 expression in infiltrating Treg cells, we sorted CD45<sup>high</sup>CD11b<sup>+</sup> macrophages and CD45<sup>low</sup>CD11b<sup>+</sup> microglia from the ipsilateral hemispheres after MCAO (Fig. 4a). These cells were then co-cultured with splenic Treg cells for 24 h before evaluation of Sirt2 expression in Treg cells. As shown in Fig. 4b, brain macrophages did not induce Sirt2 expression, whereas post-MCAO microglia effectively induced Sirt2 expression in Treg cells. This effect was also confirmed by Western blot (Fig. 4c). Furthermore, when post-MCAO microglia were cultured with Treg cells in a

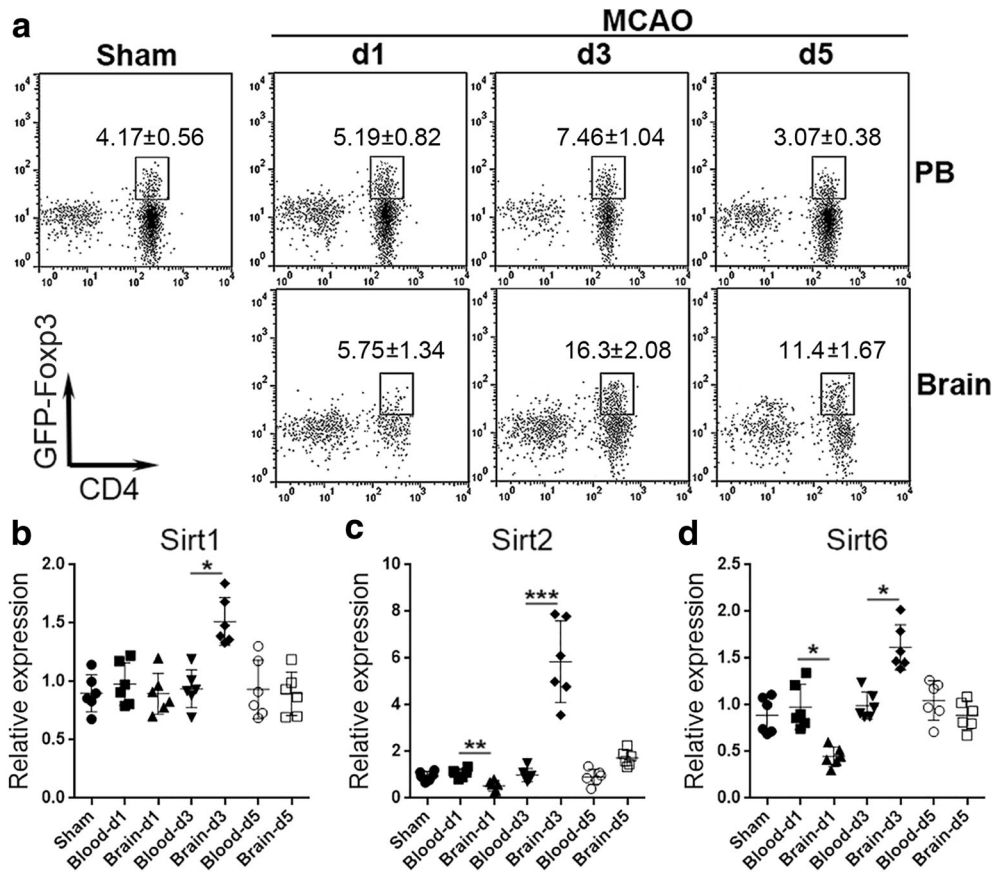


**Fig. 1.** Sirt2 expression is upregulated in infiltrating Treg cells after MCAO. **a** Representative flow cytometry dot plots showing the proportions of Foxp3-GFP<sup>+</sup> Treg cells in total T cells isolated from peripheral blood or ipsilateral hemispheres at indicated time points after MCAO. Sham, sham control. d1, day 1 after MCAO. d2, day 2 after MCAO. d3, day 3 after MCAO. *N* = 6 mice per group. **b** to **d** The relative mRNA abundances of Sirt1, Sirt2, and Sirt6 in blood Treg cells and infiltrating Treg cells. *N* = 6 mice per group. \**p* < 0.05; \*\**p* < 0.01; \*\*\**p* < 0.001.

Transwell plate, they were unable to induce Sirt2 expression in Treg cells (Fig. 4d). Therefore, post-MCAO microglia induce Sirt2 expression in Treg cells depending on cell-cell contact. Neither microglia nor macrophages induced Sirt1 or Sirt6 expression (Fig. S7).

**Post-MCAO Microglia Induce Sirt2 Expression Through HIF-1 $\alpha$**

It has been reported that HIF-1 $\alpha$  and HIF-2 $\alpha$  promote Sirt1 expression [14]. To check if HIF-1 proteins upregulate Sirt2 expression in Treg cells, we tested the protein levels of HIF-1 $\alpha$  and HIF-2 $\alpha$  in Treg cells after co-culture with post-MCAO microglia. As indicated in Fig. 5a, microglia upregulated HIF-1 $\alpha$  expression in Treg cells in a time-dependent manner. There was also a mild increase in HIF-2 $\alpha$  expression after co-culture. Microglia did not influence the expression of forkhead box protein O1

(Foxo1) and forkhead box O3 (Foxo3) which are also related to sirtuin expression (Fig. 5b). To confirm the role of HIF-1 $\alpha$  in Sirt2 expression, the selective HIF-1 $\alpha$  inhibitor PX-478 was used to pretreat Treg cells prior to co-culture with microglia. PX-478 effectively diminished microglia-induced upregulation of Sirt2 in Treg cells (Fig. 5b), suggesting that HIF-1 $\alpha$  indeed participates in microglia-induced Sirt2 expression.

**DISCUSSION**

Sirt2 deacetylates internal lysines on multiple proteins including transcription factors [15]. In this study, we focused on the expression and function of Sirt2 in infiltrating Treg cells after MCAO. We found that Sirt2 was profoundly upregulated in infiltrating Treg cells. Treg cells can

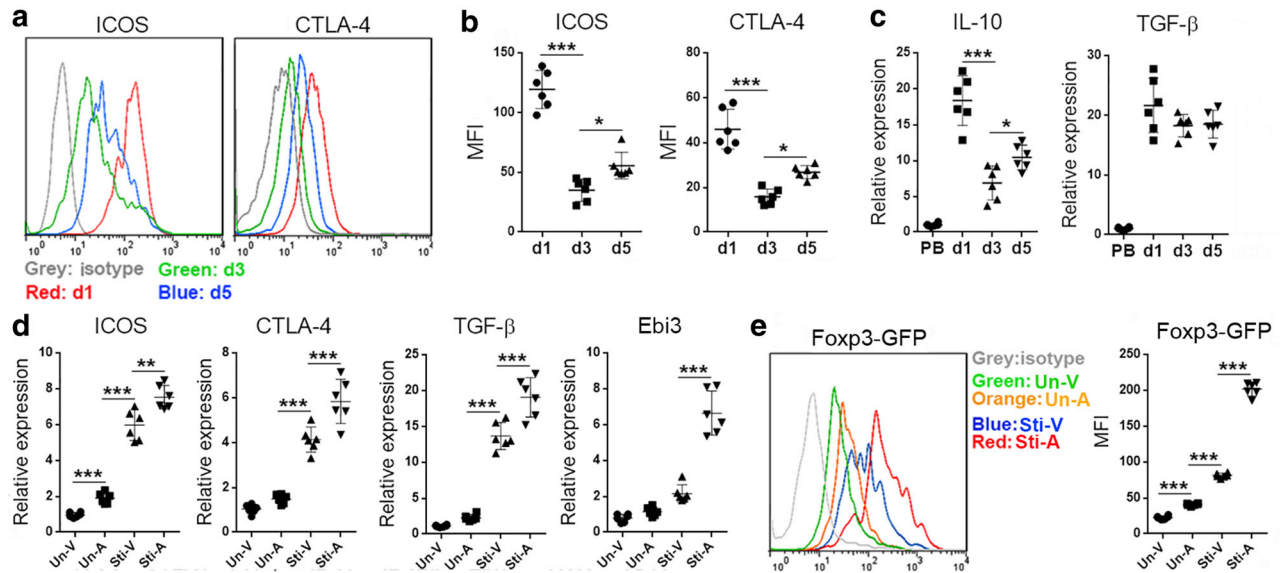


**Fig. 2.** Sirt2 inhibits the immunosuppressive function of Treg cells. **a** and **b** The expression of ICOS and CTLA-4 on infiltrating Treg cells. The representative flow cytometry histograms are shown in **(a)**. The statistics are shown in **(b)**. Isotype: isotype antibody control. d1, day 1 after MCAO. d2, day 2 after MCAO. d3, day 3 after MCAO.  $N = 6$  mice per group. **c** The mRNA abundances of IL-10 and TGF- $\beta$  in infiltrating Treg cells. PB: peripheral blood Treg cells as the control.  $N = 6$  mice per group. **d** The mRNA abundances of immunosuppression-associated molecules in infiltrating Treg cells after *in vitro* stimulation with agonistic antibodies in the presence or absence of Sirt2 inhibitor AGK2. Un, unstimulated cells. Vi, stimulated cells. V, vehicle. A, AGK2.  $N = 6$  per group. **e** The fluorescent intensity of Foxp3-GFP in infiltrating Treg cells after *in vitro* stimulation in the presence or absence of Sirt2 inhibitor AGK2. Left panel: representative histograms. Right panel: statistics of mean fluorescent intensity (MFI).  $N = 6$  per group. \* $p < 0.05$ ; \*\* $p < 0.01$ ; \*\*\* $p < 0.001$ .

control the post-stroke neuroinflammation and protect neurons from secondary injury [5]. The increase in Sirt2 expression might be a regulatory mechanism of infiltrating Treg cell activity in ischemic brains. Indeed, we revealed that Sirt2 inhibitor AGK2 enhanced the expression of immunosuppression-associated molecules and Foxp3 in cultured infiltrating Treg cells. However, the exact mechanisms underlying these changes remain unclear. It has been indicated that Sirt2 inhibits NF- $\kappa$ B activity through p65 deacetylation [15], and NF- $\kappa$ B signaling is a key regulator of Foxp3 expression during Treg cell development [16]. Hence, it is likely that Sirt2 inhibits Foxp3 expression *via* impairing NF- $\kappa$ B activity in infiltrating Treg cells. In addition, Sirt2 is required for optimal AKT activation [17] and AKT signaling blocks Foxp3 expression [18]. However, Sirt2 can directly deacetylated Foxo1 and Foxo3 to increase the transcription activity of Foxos [19, 20]. Foxo1 and Foxo3 positively regulate Foxp3 expression [21]. Therefore, further research is needed to elucidate the relationship between Sirt2 and Foxp3.

Another important discovery in this study is that post-MCAO microglia induce Sirt2 expression in Treg cells. The interactions between microglia and Treg cells have

been previously summarized [22]. Particularly, MHC-II<sup>+</sup>CD40<sup>dim</sup>CD86<sup>dim</sup>IL-10<sup>+</sup> microglia induce Ag-specific CD4<sup>+</sup>Foxp3<sup>+</sup> Treg cells [23]. However, our data suggest that reactive microglia might suppress Treg cell function in ischemic brains. The disparity between the two studies might be due to the microglia used. MHC-II<sup>+</sup>CD40<sup>dim</sup>CD86<sup>dim</sup>IL-10<sup>+</sup> microglia are likely anti-inflammatory M2 type microglia, while the microglia in our study were reactive microglia at day 3 after MCAO. In the acute phase of ischemia, microglia are polarized into pro-inflammatory M1 type cells [24]. Hence, M1 and M2 microglia might exert distinct effects on Treg cells. To our knowledge, we are the first to report the regulatory effect of post-MCAO microglia on Treg cells.

We further found that HIF-1 $\alpha$  was responsible for the induction of Sirt2 in Treg cells. HIF-1 $\alpha$  is a transcription factor that is induced under hypoxia condition or growth factor stimulation [25]. It has been implicated that Sirt1 is the downstream target gene of HIF-1 $\alpha$  [14]. HIF-1 $\alpha$  would also act as a transcription factor of Sirt2. Our ongoing study is testing if HIF-1 $\alpha$  could enhance the *Sirt2* gene promoter activity. Additionally, it is reported that *Sirt2* gene is a downstream target of serum response factor [26]. HIF-1 $\alpha$

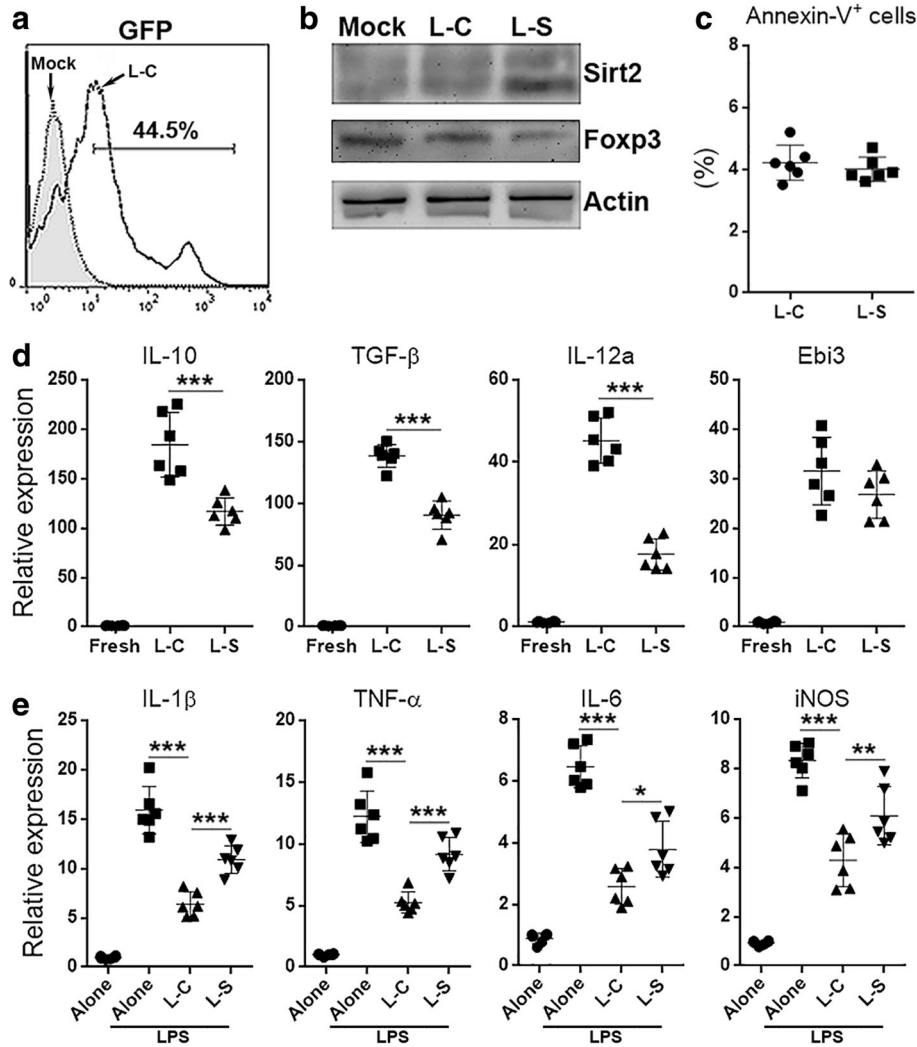


**Fig. 3.** Expression of exogenous Sirt2 suppresses the anti-inflammatory activity of Treg cells. **a** The flow cytometry histograms showing GFP expression at day 2 after lentiviral transduction. Mock, mock transduction. L-C, L-C transduction. This is a representative image of two independent experiments. **b** The protein levels of Sirt2 and Foxp3 in Treg cells. Mock, mock transduction. L-C, L-C-transduced Treg cells. L-S, L-S-transduced Treg cells. This is a representative image of two independent experiments. **c** Treg cell apoptosis at day 2 after lentiviral transduction. *N* = 6 per group. **d** The mRNA levels of indicated cytokines at day 2 after lentiviral transduction. Fresh, freshly enriched Treg cells. *N* = 6 per group. **e** The mRNA levels of indicated pro-inflammatory mediators in LPS-activated macrophages after 24-h co-culture with Treg cells. Alone-V, macrophages alone with vehicle (PBS) treatment. LPS, LPS treatment. Alone, macrophages alone. L-C, macrophages co-cultured with L-C-transduced Treg cells. L-S, macrophages co-cultured with L-S-transduced Treg cells. *N* = 6 per group. \**p* < 0.05; \*\**p* < 0.01; \*\*\**p* < 0.001.

perhaps upregulates serum response factor and indirectly induces Sirt2 expression.

Although we thought Treg cells are beneficial for stroke recovery, however, the role of Treg cells in ischemic stroke is under debate. Liesz et al. showed that Treg cells prevent secondary neurodegenerative damage following ischemic strike, and histone deacetylase inhibition can boost Treg cells

to alleviate post-ischemic neuroinflammation and thereby improve stroke outcome [27, 28]. Xie et al. also demonstrate that enhancing the anti-inflammation activity of Tregs can attenuate secondary injury and motor deficits after focal ischemia by to restrain post-stroke neuroinflammation [29, 30]. Consistently, Treg depletion or Foxp3 knockout (Foxp3-KO) failed to mitigate stroke outcome [28, 31]. Other research



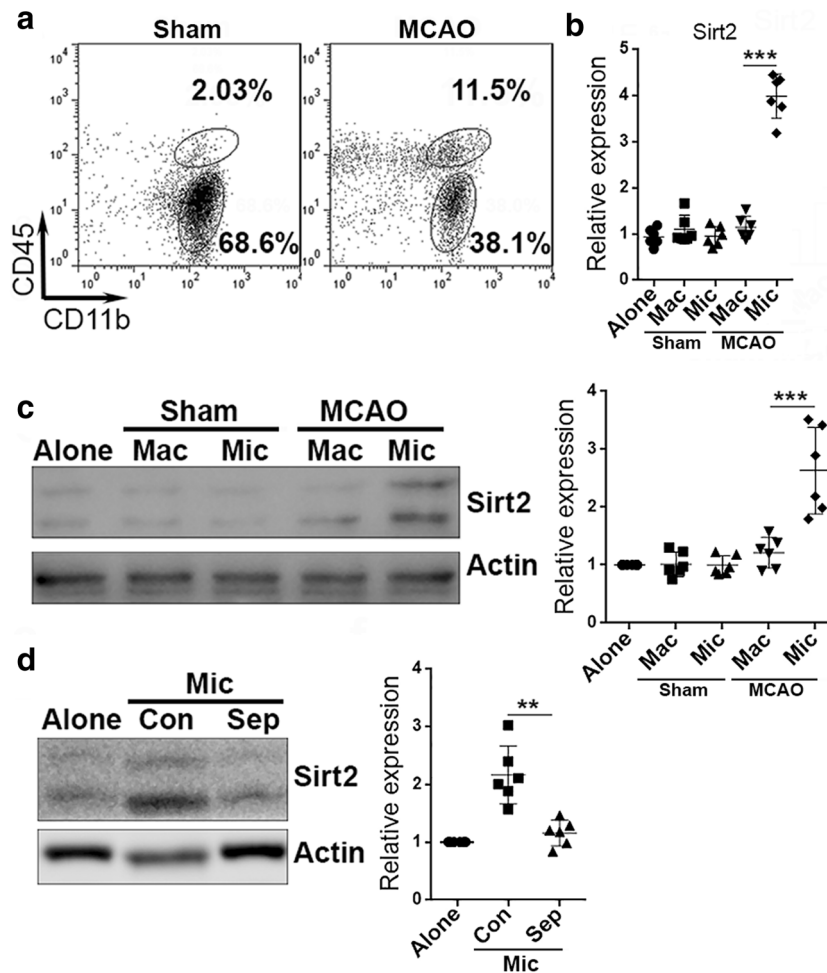


**Fig. 4.** Post-MCAO microglia induce Sirt2 expression in Treg cells. **a** The gating strategy for CD45<sup>high</sup>CD11b<sup>+</sup> macrophages and CD45<sup>low</sup>CD11b<sup>+</sup> microglia in sham-operated or MCAO-operated mice. Data are the representative of 3 independent experiments. **b** Sirt2 mRNA levels in Treg cells after co-culture with sorted macrophages and microglia. Alone, Treg cells cultured alone. Mac, Treg cells co-cultured with macrophages. Mic, Treg cells co-cultured with microglia. Sham, cells from sham-operated mice. MCAO, cells from MCAO-operated mice. *N* = 6 per group. **c** Sirt2 protein levels in Treg cells after co-culture with sorted macrophages and microglia. Left panel: representative blots. Right panel: statistics. *N* = 6 per group. **d** Sirt2 protein levels in Treg cells after culture with post-MCAO microglia in a Transwell plate. Mic, Treg cells cultured with microglia. Con, co-culture with cell-to-cell contact. Sep, separate culture without cell-to-cell contact. Left panel: representative blots. Right panel: statistics. *N* = 6 per group. \*\**p* < 0.01; \*\*\**p* < 0.001.

including adoptive transfer studies also suggest that Treg cells are neuroprotective after ischemic stroke [32–34]. However, several studies using a genetic mouse model of inducible Treg depletion illustrate either no effect or even a detrimental effect of Treg cells in the stroke models [35–37]. It is likely that such discrepancy is due to the differences in stroke models, methods of Treg depletion, and dynamics of post-stroke immune responses [6]. In addition, it would be interesting to test Sirt2 expression in different models, because the variations of Sirt2

expression might contribute to contradictory Treg cell functions. If Sirt2 expression is suppressed in the infiltrating Treg cells, these cells could be more neuroprotective since they can produce more anti-inflammatory cytokines. However, if Sirt2 expression is normal or even upregulated in Treg cells in some models, the neuroprotective activity of Treg cells could be inhibited or even abolished, and the detrimental effect of Treg cells would dominate.

In the current study, we showed that post-MCAO microglia increased Sirt2 expression in Treg cells to inhibit

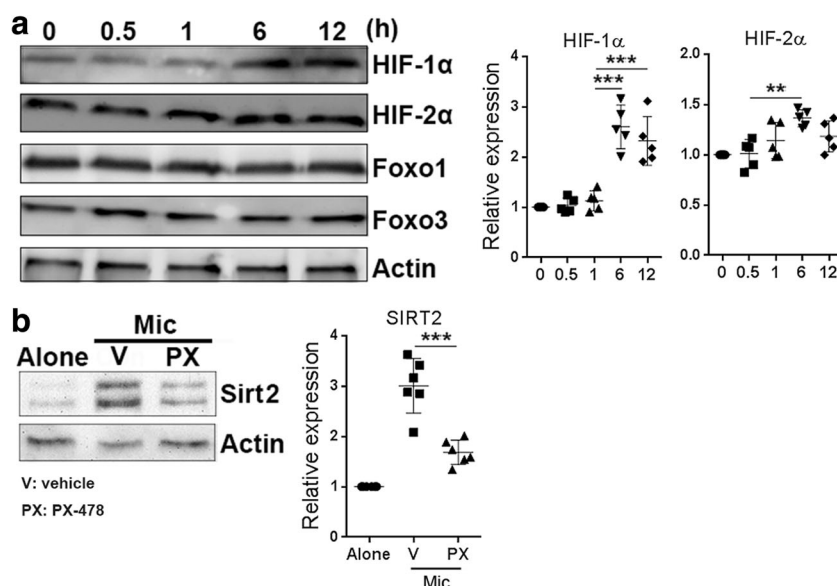


**Fig. 5.** Microglia induce Sirt2 expression *via* HIF-1 $\alpha$ . **a** The expression of HIF-1 $\alpha$ , HIF-2 $\alpha$ , Foxo1, and Foxo3 in Treg cells after co-culture with post-MCAO microglia. Left panel: representative blots. Right panel: statistics for HIF-1 $\alpha$  and HIF-2 $\alpha$  expression. *N* = 5 per group. **b** Sirt2 expression in Treg cells after co-culture with post-MCAO microglia in the presence or absence of HIF-1 $\alpha$  inhibitor PX-478. Left panel: representative blots. Right panel: statistics. Alone, Treg cells cultured alone. Mic, Treg cells co-cultured with microglia. V, vehicle. PX, PX-478. *N* = 6 per group. **\*\****p* < 0.01; **\*\*\****p* < 0.001.

Treg cell function. This raises an interesting question that whether microglia induce Sirt2 expression in conventional T cells. If yes, what is the effect of Sirt2 upregulation on invading conventional T cells? Microglia are considered the main antigen-presenting cells in the brain parenchyma during neurodegeneration [22]. Although the evidence showing that microglia present CNS antigens to infiltrating T cells is still in lack, this possibility cannot be ruled out due to the biology of microglia and T cells. It is now acknowledged that microglia are equipped with machinery needed for antigen presentation, and they might present CNS antigens to infiltrating T cells during experimental autoimmune encephalomyelitis [38, 39]. In addition, clonal T cell expansion has been found in ischemic brains, suggesting that some invading T cells might be activated *via* TCR signaling [40]. If infiltrating T cells are activated by microglia-mediated presentation of CNS antigens, autoreactive T cells might chronically proliferate and impair the neurons, oligodendrocytes, and astrocytes even when ischemia is over. The upregulation of Sirt2 could counteract the activation of autoreactive T cells, since Sirt2 can represses NFAT transcription factor [41]. NFAT is a key factor of TCR-calcium-calcineurin-NFAT pathway which leads to T cell activation [42]. However, this hypothesis needs to be tested in further studies.

### FUNDING INFORMATION

This study was supported by the Natural Science Foundation of Hubei Province (Grant No. WJ2017X020).

### COMPLIANCE WITH ETHICAL STANDARDS

**Conflict of Interest.** The authors declare that they have no conflict of interest.

### REFERENCES

1. Kokaia, Z., 2015. Targeting neuroinflammation for treatment of ischemic stroke. *Georgian Medical News* 84–87.
2. Kawabori, M., and M.A. Yenari. 2015. Inflammatory responses in brain ischemia. *Current Medicinal Chemistry* 22: 1258–1277.
3. Kleinschnitz, C., N. Schwab, P. Kraft, I. Hagedorn, A. Dreykluft, T. Schwarz, M. Austinat, B. Nieswandt, H. Wiendl, and G. Stoll. 2010. Early detrimental T-cell effects in experimental cerebral ischemia are neither related to adaptive immunity nor thrombus formation. *Blood* 115: 3835–3842.
4. Iadecola, C., and J. Anrather. 2011. The immunology of stroke: From mechanisms to translation. *Nature Medicine* 17: 796–808.
5. Chen, S., H. Wu, D. Klebe, Y. Hong, J. Zhang, and J. Tang. 2013. Regulatory T cell in stroke: A new paradigm for immune regulation. *Clinical & Developmental Immunology* 2013: 689827.

6. Xia, Y., W. Cai, A.W. Thomson, and X. Hu. 2016. Regulatory T cell therapy for ischemic stroke: How far from clinical translation? *Translational Stroke Research* 7: 415–419.
7. Sidorova-Darnos, E., R.G. Wither, N. Shulyakova, C. Fisher, M. Ratnam, M. Aarts, L. Lilje, P.P. Monnier, and J.H. Eubanks. 2014. Differential expression of sirtuin family members in the developing, adult, and aged rat brain. *Frontiers in Aging Neuroscience* 6: 333.
8. Zhang, J., S.M. Lee, S. Shannon, B. Gao, W. Chen, A. Chen, R. Divekar, M.W. McBurney, H. Braley-Mullen, H. Zaghouni, and D. Fang. 2009. The type III histone deacetylase Sirt1 is essential for maintenance of T cell tolerance in mice. *The Journal of Clinical Investigation* 119: 3048–3058.
9. Zou, T., Y. Yang, F. Xia, A. Huang, X. Gao, D. Fang, S. Xiong, and J. Zhang. 2013. Resveratrol inhibits CD4+ T cell activation by enhancing the expression and activity of Sirt1. *PLoS One* 8: e75139.
10. Beier, U.H., L. Wang, T.R. Bhatti, Y. Liu, R. Han, G. Ge, and W.W. Hancock. 2011. Sirtuin-1 targeting promotes Foxp3+ T-regulatory cell function and prolongs allograft survival. *Molecular and Cellular Biology* 31: 1022–1029.
11. van Loosdregt, J., D. Brunen, V. Fleskens, C.E. Pals, E.W. Lam, and P.J. Coffey. 2011. Rapid temporal control of Foxp3 protein degradation by sirtuin-1. *PLoS One* 6: e19047.
12. Kwon, H.S., H.W. Lim, J. Wu, M. Schnolzer, E. Verdin, and M. Ott. 2012. Three novel acetylation sites in the Foxp3 transcription factor regulate the suppressive activity of regulatory T cells. *Journal of Immunology* 188: 2712–2721.
13. Chiang, T., Messing, R. O. and Chou, W. H.. 2011. Mouse model of middle cerebral artery occlusion. *Journal of Visualized Experiments*.
14. Qin, J., Y. Liu, Y. Lu, M. Liu, M. Li, J. Li, and L. Wu. 2017. Hypoxia-inducible factor 1 alpha promotes cancer stem cells-like properties in human ovarian cancer cells by upregulating SIRT1 expression. *Scientific Reports* 7: 10592.
15. Gomes, P., T. Fleming Outeiro, and C. Cavadas. 2015. Emerging role of sirtuin 2 in the regulation of mammalian metabolism. *Trends in Pharmacological Sciences* 36: 756–768.
16. Long, M., S.G. Park, I. Strickland, M.S. Hayden, and S. Ghosh. 2009. Nuclear factor-kappaB modulates regulatory T cell development by directly regulating expression of Foxp3 transcription factor. *Immunity* 31: 921–931.
17. Ramakrishnan, G., G. Davaakhuu, L. Kaplun, W.C. Chung, A. Rana, A. Atfi, L. Miele, and G. Tzivion. 2014. Sirt2 deacetylase is a novel AKT binding partner critical for AKT activation by insulin. *The Journal of Biological Chemistry* 289: 6054–6066.
18. Kasper, I.R., S.A. Apostolidis, A. Sharabi, and G.C. Tsokos. 2016. Empowering regulatory T cells in autoimmunity. *Trends in Molecular Medicine* 22: 784–797.
19. Daitoku, H., J. Sakamaki, and A. Fukamizu. 2011. Regulation of FoxO transcription factors by acetylation and protein-protein interactions. *Biochimica et Biophysica Acta* 1813: 1954–1960.
20. Wang, F., M. Nguyen, F.X. Qin, and Q. Tong. 2007. SIRT2 deacetylates FOXO3a in response to oxidative stress and caloric restriction. *Aging Cell* 6: 505–514.
21. Ohkura, N., and S. Sakaguchi. 2010. Foxo1 and Foxo3 help Foxp3. *Immunity* 33: 835–837.
22. Schettlers, S.T.T., D. Gomez-Nicola, J.J. Garcia-Vallejo, and Y. Van Kooyk. 2017. Neuroinflammation: Microglia and T cells get ready to tango. *Frontiers in Immunology* 8: 1905.
23. Ebner, F., C. Brandt, P. Thiele, D. Richter, U. Schliesser, V. Siffrin, J. Schueler, T. Stubbe, A. Ellinghaus, C. Meisel, B. Sawitzki, and R. Nitsch. 2013. Microglial activation milieu controls regulatory T cell responses. *Journal of Immunology* 191: 5594–5602.
24. Cherry, J.D., J.A. Olschowka, and M.K. O'Banion. 2014. Neuroinflammation and M2 microglia: The good, the bad, and the inflamed. *Journal of Neuroinflammation* 11: 98.
25. Strieter, R.M. 2005. Masters of angiogenesis. *Nature Medicine* 11: 925–927.
26. Zhang, X., G. Azhar, and J.Y. Wei. 2017. SIRT2 gene has a classic SRE element, is a downstream target of serum response factor and is likely activated during serum stimulation. *PLoS One* 12: e0190011.
27. Liesz, A., E. Suri-Payer, C. Veltkamp, H. Doerr, C. Sommer, S. Rivest, T. Giese, and R. Veltkamp. 2009. Regulatory T cells are key cerebroprotective immunomodulators in acute experimental stroke. *Nature Medicine* 15: 192–199.
28. Liesz, A., W. Zhou, S.Y. Na, G.J. Hammerling, N. Garbi, S. Karcher, E. Mratsko, J. Backs, S. Rivest, and R. Veltkamp. 2013. Boosting regulatory T cells limits neuroinflammation in permanent cortical stroke. *The Journal of Neuroscience* 33: 17350–17362.
29. Xie, L., F. Sun, J. Wang, X. Mao, L. Xie, S.H. Yang, D.M. Su, J.W. Simpkins, D.A. Greenberg, and K. Jin. 2014. mTOR signaling inhibition modulates macrophage/microglia-mediated neuroinflammation and secondary injury via regulatory T cells after focal ischemia. *Journal of Immunology* 192: 6009–6019.
30. Xie, L., G.R. Choudhury, A. Winters, S.H. Yang, and K. Jin. 2015. Cerebral regulatory T cells restrain microglia/macrophage-mediated inflammatory responses via IL-10. *European Journal of Immunology* 45: 180–191.
31. Stubbe, T., F. Ebner, D. Richter, O. Engel, J. Klehmet, G. Royl, A. Meisel, R. Nitsch, C. Meisel, and C. Brandt. 2013. Regulatory T cells accumulate and proliferate in the ischemic hemisphere for up to 30 days after MCAO. *Journal of Cerebral Blood Flow and Metabolism* 33: 37–47.
32. Li, P., Y. Gan, B.L. Sun, F. Zhang, B. Lu, Y. Gao, W. Liang, A.W. Thomson, J. Chen, and X. Hu. 2013. Adoptive regulatory T-cell therapy protects against cerebral ischemia. *Annals of Neurology* 74: 458–471.
33. Zhang, H., Y. Xia, Q. Ye, F. Yu, W. Zhu, P. Li, Z. Wei, Y. Yang, Y. Shi, A.W. Thomson, J. Chen, and X. Hu. 2018. In vivo expansion of regulatory T cells with IL-2/IL-2 antibody complex protects against transient ischemic stroke. *The Journal of Neuroscience* 38: 10168–10179.
34. Brea, D., J. Agulla, M. Rodriguez-Yanez, D. Barral, P. Ramos-Cabrer, F. Campos, A. Almeida, A. Davalos, and J. Castillo. 2014. Regulatory T cells modulate inflammation and reduce infarct volume in experimental brain ischaemia. *Journal of Cellular and Molecular Medicine* 18: 1571–1579.
35. Ren, X., K. Akiyoshi, A.A. Vandenbark, P.D. Hurn, and H. Offner. 2011. CD4+FoxP3+ regulatory T-cells in cerebral ischemic stroke. *Metabolic Brain Disease* 26: 87–90.
36. Kleinschnitz, C., P. Kraft, A. Dreykluft, I. Hagedorn, K. Gobel, M.K. Schuhmann, F. Langhauser, X. Helluy, T. Schwarz, S. Bittner, C.T. Mayer, M. Brede, C. Varallyay, M. Pham, M. Bendzus, P. Jakob, T. Magnus, S.G. Meuth, Y. Iwakura, A. Zernecke, T. Sparwasser, B. Nieswandt, G. Stoll, and H. Wiendl. 2013. Regulatory T cells are strong promoters of acute ischemic stroke in mice by inducing dysfunction of the cerebral microvasculature. *Blood* 121: 679–691.
37. Schuhmann, M.K., P. Kraft, G. Stoll, K. Lorenz, S.G. Meuth, H. Wiendl, B. Nieswandt, T. Sparwasser, N. Beyersdorf, T. Kerkau, and C. Kleinschnitz. 2015. CD28 superagonist-mediated boost of regulatory T cells increases thrombo-inflammation and ischemic neurodegeneration during the acute phase of experimental stroke. *Journal of Cerebral Blood Flow and Metabolism* 35: 6–10.

38. Almolda, B., B. Gonzalez, and B. Castellano. 2011. Antigen presentation in EAE: Role of microglia, macrophages and dendritic cells. *Frontiers of Biology (Landmark Ed)* 16: 1157–1171.
39. Wlodarczyk, A., M. Lobner, O. Cedile, and T. Owens. 2014. Comparison of microglia and infiltrating CD11c(+) cells as antigen presenting cells for T cell proliferation and cytokine response. *Journal of Neuroinflammation* 11: 57.
40. Liesz, A., S. Karcher, and R. Veltkamp. 2013. Spectratype analysis of clonal T cell expansion in murine experimental stroke. *Journal of Neuroimmunology* 257: 46–52.
41. Sarikhani, M., S. Maity, S. Mishra, A. Jain, A.K. Tamta, V. Ravi, M.S. Kondapalli, P.A. Desingu, D. Khan, S. Kumar, S. Rao, M. Inbaraj, A.S. Pandit, and N.R. Sundaresan. 2018. SIRT2 deacetylase represses NFAT transcription factor to maintain cardiac homeostasis. *The Journal of Biological Chemistry* 293: 5281–5294.
42. Macian, F. 2005. NFAT proteins: Key regulators of T-cell development and function. *Nature Reviews. Immunology* 5: 472–484.

**Publisher's Note** Springer Nature remains neutral with regard to jurisdictional claims in published maps and institutional affiliations.